Journal of Peptide Science
J. Pept. Sci. 2008; **14**: 742–754
Published online 10 January 2008 in Wiley InterScience (www.interscience.wiley.com). DOI: 10.1002/psc.992

JOURNAL OF PEPTIDE SCIENCE

Kissper, a kiwi fruit peptide with channel-like activity: Structural and functional features‡

M. ANTONIETTA CIARDIELLO,[a]* DANIELA MELELEO,[b] GABRIELLA SAVIANO,[c] ROBERTA CRESCENZO,[a] VITO CARRATORE,[a] LAURA CAMARDELLA,[a] ENRICO GALLUCCI,[b] SILVIA MICELLI,[b] TEODORICO TANCREDI,[d] DELIA PICONE[e] and MAURIZIO TAMBURRINI[a]

[a] Istituto di Biochimica delle Proteine, C.N.R., I-80131 Napoli, Italy
[b] Dipartimento Farmaco-Biologico, Università degli Studi di Bari, I-70126 Bari, Italy
[c] Dipartimento STAT, Università degli Studi del Molise, I-86170 Pesche (Is), Italy
[d] Istituto di Chimica Biomolecolare, C.N.R., I-80078 Pozzuoli (Na), Italy
[e] Dipartimento di Chimica, Università di Napoli Federico II, I-80126 Napoli, Italy

Received 19 October 2007; *Revised 31 October 2007*; *Accepted 4 November 2007*

Abstract: Kissper is a 39-residue peptide isolated from kiwi fruit (*Actinidia deliciosa*). Its primary structure, elucidated by direct protein sequencing, is identical to the *N*-terminal region of kiwellin, a recently reported kiwi fruit allergenic protein, suggesting that kissper derives from the *in vivo* processing of kiwellin. The peptide does not show high sequence identity with any other polypeptide of known function. However, it displays a pattern of cysteines similar, but not identical, to those observed in some plant and animal proteins, including toxins involved in defence mechanisms. A number of these proteins are also active on mammalian cells. Functional characterization of kissper showed pH-dependent and voltage-gated pore-forming activity, together with anion selectivity and channeling in model synthetic PLMs, made up of POPC and of DOPS : DOPE : POPC. A 2DNMR analysis indicates that in aqueous solution kissper has only short regions of regular secondary structure, without any evident similarity with other bioactive peptides. Comparative analysis of the structural and functional features suggests that kissper is a member of a new class of pore-forming peptides with potential effects on human health. Copyright © 2008 European Peptide Society and John Wiley & Sons, Ltd.

Keywords: kiwi fruit; peptide; amino acid sequence; NMR; membrane channels; ion transport

INTRODUCTION

Regular consumption of fruit and vegetables is generally associated with a reduction of the risk of several human pathologies, such as cardiovascular diseases, heart failure, microbial infections, cancer, Alzheimer's disease, cataract and other age-related functional degenerations [1–3]. These advantages are usually ascribed to rich vitamin and antioxidant and dietary fibre content, although other constituents may have beneficial effects on human health [4]. Recently, food containing significant amounts of bioactive molecules with effects beyond nutritional aspects and playing important roles in the prevention of chronic diseases has been referred to as 'functional food' [2,5]. The effects of dietary fruit and vegetables on health are yet to be fully explained, and might be associated with as yet unidentified components that are still to be characterized both chemically and functionally.

Biochemical and genetic studies have also identified several PR (Pathogenesis Related) proteins, playing a role in plant defence against pathogen agents. A number of these bioactive polypeptides have been found also in dietary plants and in some cases they show toxicity against human pathogens [6–8]. Therefore, isolation and characterization of these polypeptides could provide new insights for the production of novel drugs that are able to improve human resistance to infections.

Kiwi fruit is a food with significant effects on human health. In Chinese traditional medicine this fruit was used for the prevention and therapy of many different types of cancers [9]. More recently, a number of experimental data suggests the presence of biological activities associated to kiwi fruit extracts or to specific molecules isolated from this fruit, such as *in vitro* cytotoxicity for tumor cell lines and antimicrobial activity [9], protection against oxidative DNA damage [10] and cardiovascular protective properties [11]. Human trial data indicated that daily consumption of kiwi fruit promoted laxation in elderly people [12]. *In vitro* experiments showed that the PR protein thaumatin, isolated from kiwi fruit, displays antifungal and antiviral (anti-HIV) activities against human pathogens [13].

Abbreviations: FPLC, fast protein liquid chromatography; HSQC, heteronuclear single-quantum coherence; PLM, planar lipid membrane; POPC, palmitoyloleoylphosphatidylcholine; DOPS, dioleoylphosphatidylserine; DOPE, dioleoylphosphatidylethanolamine.

*Correspondence to: M. Antonietta Ciardiello, Istituto di Biochimica delle Proteine, CNR, Via Pietro Castellino 111, I-80131 Napoli, Italy; e-mail: ma.ciardiello@ibp.cnr.it

‡The protein sequence data reported in this paper will appear in the Swiss-Prot and TrEMBL knowledgebase under the accession number P83975.

Unfortunately, an increasing number of individuals have to avoid consumption of kiwi fruit due to the presence of several allergens [13–17]. The isolation and characterization of molecules associated with the specific biological effects of kiwi fruit appears to be an important goal, which might enlarge our knowledge about a possibly safe pharmacological use of naturally occurring drugs. In particular, a proteomic analysis of the edible portion of ripe kiwi fruit may allow the identification of the polypeptides ingested during consumption and suggest their possible biological effects.

In the framework of a proteomic study on kiwi fruit (*Actinidia deliciosa*), we have undertaken the analysis of proteins and peptides found in the ripening fruit. Kiwi fruit pectin methylesterase inhibitor [18] and pectin methylesterase [19] have already been isolated and characterized, and the study of a possible influence on human health is under investigation. More recently, we have isolated kiwellin [17], a novel allergenic protein which is one of the three most abundant proteins present in the edible part of this fruit. We report here the purification, the characterization and the complete amino acid sequence of a novel peptide (henceforth named kissper), isolated in our laboratory. Furthermore, as a planar lipid bilayer system provides an elegant way to study membrane-active compounds, electrophysiological studies have been carried out on model synthetic PLMs made up of POPC or DOPS : DOPE : POPC as a surrogate for the intestinal lipids [20], and the solution structure of the peptide has been investigated by 2D NMR. The data obtained are discussed and compared with those of kiwellin and other peptides and proteins from various families, with related structural features and/or biological activities.

MATERIALS AND METHODS

Reagents

Kiwi fruits were purchased in Italy from a local farm; they were picked in mid October and stored for a week at room temperature until slightly soft. Trypsin was from Boehringer (Mannheim, Germany); bovine serum albumin, dithiothreitol, Tris, and 4-vinylpyridine from Sigma (Milan, Italy); DEAE-cellulose (type DE52) from Whatman (Brentford, UK). HPLC-grade acetonitrile was from Baker (Phillipsburg, NJ, USA). Salts and other analytical grade basic chemicals used in PLM studies were bought from Merck (Darmstadt, FRG, analytical grade), whereas biochemicals were from Sigma. POPC was purchased from Avanti Polar Lipids (Alabaster, AL, USA). Sequencer grade reagents were from Applied Biosystems (Foster City, CA, USA). All other reagents were of the highest commercially available quality.

Protein Purification and Characterization

FPLC ion-exchange chromatography was carried out on a Mono-Q HR 10/10 column (Amersham-Pharmacia, Milan, Italy), at a flow-rate of 3 ml/min, recording the absorbance at 280 nm.

Protein concentrations were determined by the BIO-RAD Protein Assay (BIO-RAD, Segrate, Italy), using calibration curves made with bovine serum albumin. When required, protein samples were concentrated by ultrafiltration using Centriplus YM-3 filters (Amicon, Millipore, Bedford, MA, USA).

Denaturation and alkylation was carried out by dissolving the peptide at a concentration of 2 mg/ml in 0.5 M Tris-HCl pH 7.8, containing 2 mM EDTA and 6 M guanidine hydrochloride. Dithiothreitol (ten-fold molar excess over the thiol groups of the protein) was added under nitrogen atmosphere, and the solution was kept at 37 °C for 1 h. 4-vinylpyridine (five-fold molar excess over the total thiols) was then added under nitrogen atmosphere, and the mixture was kept in the dark at room temperature for 30 min. At the end of the reaction, excess reagents were removed by gel filtration on a PD-10 column (Amersham-Pharmacia) equilibrated with 0.1% TFA.

Tryptic digestions on pyridylethylated samples (0.5 mg/ml) were carried out at an enzyme : protein ratio of 1 : 20 (w : w) in 1% ammonium bicarbonate, at 37 °C for 2 h.

Reverse-phase HPLC of kiwi extracts and of peptides derived from chemical or enzymatic cleavage was performed on a Vydac (Deerfield, IL, USA) C_8 column (0.21 × 25 cm), using a Beckman (Fullerton, CA, USA) System Gold apparatus. Elution was accomplished by a multistep linear gradient of eluant B (0.08% TFA in acetonitrile) in eluant A (0.1% TFA) at a flow rate of 1 ml/min. The eluate was monitored at 220 and 280 nm. The separated fractions were manually collected and analyzed as needed.

Amino acid sequencing was performed with an Applied Biosystems Procise 492 automatic sequencer, equipped with on-line detection of phenylthiohydantoin amino acids. Protein sequence analyses were performed using softwares available on the ExPASy Proteomics Server (www.expasy.org).

MALDI-TOF mass spectrometry was carried out on a PerSeptive Biosystems (Framingham, MA, USA) Voyager-DE Biospectrometry Workstation. Analyses were performed on premixed solutions prepared by diluting samples (final concentration 5 pmol/μl) in 4 volumes of matrix, namely 10 mg/ml α–cyano-4-hydroxycinnamic acid in 60% acetonitrile containing 0.3% TFA.

NMR

NMR measurements were performed on a sample prepared by dissolving 1 mg of freeze-dried peptide in 0.60 ml of 25 mM phosphate buffer (in 90% H_2O, 10% ^2H_2O), pH 3.5. NMR spectra were acquired at 300 K using a 600 MHz Bruker (Billerica, MA, USA) DRX spectrometer equipped with a cryoprobe. 2D ^{1}H-TOCSY [21], NOESY [22] and DQF-COSY [23], as well as ^{1}H-^{13}C and ^{1}H-^{15}N-HSQC [24] spectra were used for resonance assignments. The HDO solvent resonance was suppressed using the WATERGATE pulse sequence [25]. NOESY at different mixing times were acquired for assignment and structure calculations, TOCSY experiments were recorded with mixing times of 30 and 70 ms. The $^3J_{NHC\alpha H}$ coupling constants were measured for resolved NH amidic protons from a 1D spectrum. 2D

DOI: 10.1002/psc

data were typically apodized with a Gaussian window function and zero-filled to 1 K in F_1 prior to Fourier transform. NMRPipe [26] and NMRView [27] programs were used for data processing and spectral analysis, respectively. ^{1}H chemical shifts were referenced to the water signal at 4.70 ppm, ^{15}N chemical shifts were indirectly referenced to the ^{1}H chemical shifts according to magnetogiric ratios [28].

Cross-peaks of the NOESY spectrum at 300 ms mixing time were integrated by NMRView, transferred to the program package DYANA 1.0.6 [29], and converted to upper distance limits. Structure calculation was carried out by torsion angle dynamics. Eighty structures were calculated by TSSA, starting with a total of 10 000 MD steps and a default value of maximum temperature. The 20 best structures, in terms of target function, were considered as models of the solution structure of kissper.

Planar Membrane Experiments

PLMs were composed of POPC or of DOPS : DOPE : POPC (27 : 27:18, w : w : w) in 1% *n*-decane and formed as previously described [30]. The measurements were carried out at pH 7.0, or at pH 3.5, and at 22 ± 1 °C. Bilayers were painted across a 0.3 mm diameter circular hole in a teflon divider separating two 4 ml teflon chambers. The membrane current was monitored with an oscilloscope and recorded on a chart recorder for data analysis. The *cis* and *trans* chambers were connected to the amplifier head stage by Ag/AgCl electrodes in series with a voltage source and a highly sensitive current amplifier. The single-channel instrumentation had a time resolution of 1–10 ms, depending on the magnitude of the single-channel conductance. The *cis*-side compartment, where kissper was added, had a positive polarity. The painted PLMs were tested for integrity by checking the reflectance optically and also by their resistance and capacitance. After the membranes were formed, 4 or 8 µl of a 40 µg/ml kissper solution in bidistilled water at pH 3.8 were added on the *cis* compartment and stirred to reach a final concentration of 0.04 and 0.08 µg/ml. To allow comparison of the results, particular attention was devoted to the standardization of the experimental conditions, such as (i) volume of the cell, (ii) stirring of the bathing solutions and (iii) modality of peptide addition.

The channel incorporation was studied as follows: (i) To define the mean channel conductance (central conductance Λ_c), the single-channel data were obtained from at least three experiments with usually more than 150 single events for each series performed on different days. Upward/downward (positive/negative applied voltage, respectively) current transition (event) was more frequent than terminating events. A histogram of the current amplitude distribution for each experiment was constructed and fitted by a Gaussian distribution function (GraphPad Prism version 3.0; GraphPad Software, Inc, http://www.graphpad.com). (ii) To identify the charge of the ion carrying the current, we measured the shift in the reversal potential induced by a change from a symmetrical to an asymmetrical KCl solution system. When the membrane conductance reached a virtually stable value, after kissper addition on the *cis* side, the salt concentration on the *cis* side of the membrane was raised by the addition of a concentrated salt solution. A salt concentration gradient was set, with 1.5 M on one side (*cis*) and 0.3–1 M on the other (*trans*) (pH 7.0 and 3.5, respectively), in POPC PLM. In DOPS : DOPE : POPC PLM the concentration gradient was 1.0 M on the *cis* side and 0.5 M on the *trans* side. The reversal potential was determined by changing the holding potential step by step by ±2 mV. The permeability ratio was calculated using the Hodgkin-Goldman-Katz equation [31]:

$$V = (RT/F) \times \ln \{(P_K[K]_t + P_{Cl}[Cl]_c)/(P_K[K]_c + P_{Cl}[Cl]_t)\}$$

where $[X]_t$ and $[X]_c$ are the concentrations of the ion species X in the *trans* and *cis* compartments, respectively; R, T and F have their usual meanings.

In all the experiments that were performed, the conductance and capacitance of each membrane were tested by applying a voltage of ±200 mV for 10–15 min under stirring, to ensure that the membrane was stable. In all sets of experiments, the initial applied voltage was 80 mV and, if the channel insertion did not occur within 1 h, it was increased step by step until the first channel-like activity appeared (activation voltage and activation time). Then, the voltage could be lowered or increased and the voltage dependence studied at different voltage values. Results are expressed as means ± SE. Statistical significance was assessed using Students' *t*-tests.

RESULTS

Isolation and Purification of Kissper

Ripe kiwi fruits were peeled and washed, and then homogenized in water (1 : 1, mass/vol). The pH of the homogenate was 3.5. After centrifugation at 10 400*g* for 20 min, the supernatant, representing the soluble fraction, was collected. Large proteins were precipitated with 0.1% TFA, at 0–4 °C for 30 min, and then removed by centrifugation at 12 100*g* for 20 min. An aliquot of the supernatant was analyzed by reverse-phase HPLC, as described under Materials and Methods, and the *N*-terminal amino acid sequence of several collected fractions was established by automated sequencing. Upon comparative analysis, one of the components (kissper) showed the same *N*-terminal sequence of

DOI: 10.1002/psc

kiwellin [17], the kiwi fruit allergenic protein previously isolated and characterized.

In order to purify larger amounts of kissper, the supernatant obtained upon precipitation of the soluble fraction with TFA was dialyzed in 3500 Da MW cut-off tubings against 10 mM Tris-HCl, pH 8.0, and then loaded on a DE52 column (2.5 × 18 cm), equilibrated in the same buffer. The column was eluted with 0.5 M NaCl in the equilibrating buffer, and aliquots of the collected fractions were analyzed by reverse-phase HPLC. The fractions containing kissper were dialyzed against 10 mM Tris-HCl, pH 8.0, and then loaded on a Mono-Q HR 10/10 column, equilibrated in the same buffer. The column was eluted by a linear gradient from 0 to 0.3 M NaCl. The fractions from Mono-Q were analyzed by reverse-phase HPLC, and those containing kissper were concentrated by ultrafiltration. If needed, kissper was additionally purified to homogeneity by reverse-phase HPLC. Up to 3 mg of pure peptide was obtained from 300 g of ripe kiwi fruits.

Amino Acid Sequence

N-Terminal amino acid sequencing of kissper proceeded for 30 residues. After denaturation and alkylation of the sulfhydryl groups, kissper was digested with trypsin as described earlier, and the resulting peptides were analyzed by reverse-phase HPLC. The peaks were collected manually, vacuum-dried, redissolved in 0.1% TFA containing 20% acetonitrile and sequenced. The sequence established by alignment of the tryptic peptides with the sequence obtained from the *N*-terminus of intact kissper and with the sequence of kiwellin [17] corresponded to a 37-residue peptide, with Arg at the *C*-terminus, and accounting for a molecular weight of 3992.5 Da, whereas that obtained by MALDI-TOF mass spectrometry was 4154 Da. However, as shown in more detail below, this apparent contradiction was resolved by NMR analysis, since in the 2D spectra we were able to clearly identify the spin systems of 39 residues, including Gly38 and Thr39, following Arg37 in the primary structure of kiwellin and kissper, that were lost in the HPLC purification subsequent the trypsin cleavage. The molecular weight calculated for the complete sequence, containing 39 amino acid residues (Figure 1), was 4150.6 Da, in good agreement with that obtained by MALDI-TOF mass spectrometry. The amino acid sequence of kissper contained six cysteine residues and only one aromatic residue (His34).

Homology searches were carried out by using the Fasta3 Program. Search in the UniProt Data Bank showed the highest identity (69%) with the *N*-terminal region of both the putative kiwellin from potato leaves (UNIPROT accession number Q2HPL5) and the cDNA-derived sequence of Grip 22 from grape [32]. Search in the Swiss-Prot Data Bank, carried out using default parameters, showed from 31 to 47% sequence identities

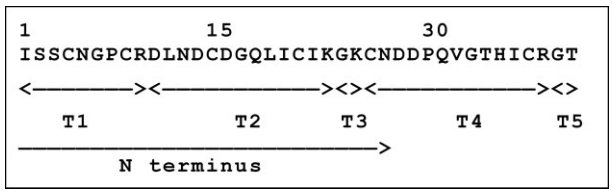

Figure 1 Amino acid sequence of kissper. The tryptic peptides (T1–T5) and the sequence portion elucidated by automated Edman degradation from the *N*-terminus are indicated below the sequence.

with the corresponding overlapping regions of several peptides and of small, as well as large, proteins (Figure 2) having a variety of functions, such as toxins (from scorpion, mollusc, snake and spider), protease inhibitors and other proteins containing the EGF-like cysteine-rich motif [33], including fibrillin, transforming growth factor and thrombomodulin.

Chemical Characterization of Disulfide Bridges

Digestion of 8 μg of native kissper was attempted (i) dissolving the sample in 20 μl of 5% formic acid, and incubating with pepsin at an enzyme : peptide ratio of 1 : 25 (w : w) at 37 °C for 2 h, and (ii) dissolving the sample in 20 μl of 1% ammonium bicarbonate, and incubating with trypsin at an enzyme : peptide ratio of 1 : 20 (w : w) at 37 °C for 2 h. Both hydrolysates were analyzed by reverse-phase HPLC, where the sample was eluted in a single peak at the same retention time of kissper, and by amino acid sequencing, where only the *N*-terminal sequence of kissper was observed. Therefore, the two digestions were ineffective.

Following an alternative strategy, an aliquot of kissper (16 μg) was dissolved in 50 μl of 70% formic acid, and incubated at 42 °C for 20 h to specifically cleave the Asp28-Pro29 bond of the sequence. After incubation, HPLC analysis (carried out as described earlier) showed only one peak, eluted at 26.7 min (not shown), whereas two amino acid sequences were determined, one proceeding from the *N*-terminal Ile and another proceeding from Pro29, in a molar ratio of 2 : 1, respectively, indicating that only 50% of kissper had been cleaved. After drying under vacuum, the sample was redissolved in water and dried again two times, in order to remove the residual acid, and then incubated with trypsin, as described above, for 5 h. Two peaks were obtained upon HPLC analysis (not shown). The peptide eluted at the retention time 26.7 min contained only the *N*-terminal amino acid sequence of kissper, whereas the one eluted at 27.3 min contained three sequences, proceeding from Ile1, Gly23 and Pro29, respectively. This result suggests that only the sample previously cleaved by the acidic treatment could be hydrolyzed by trypsin. The sample eluted at 27.3 min was successively dried under vacuum, and then incubated with pepsin, as

DOI: 10.1002/psc

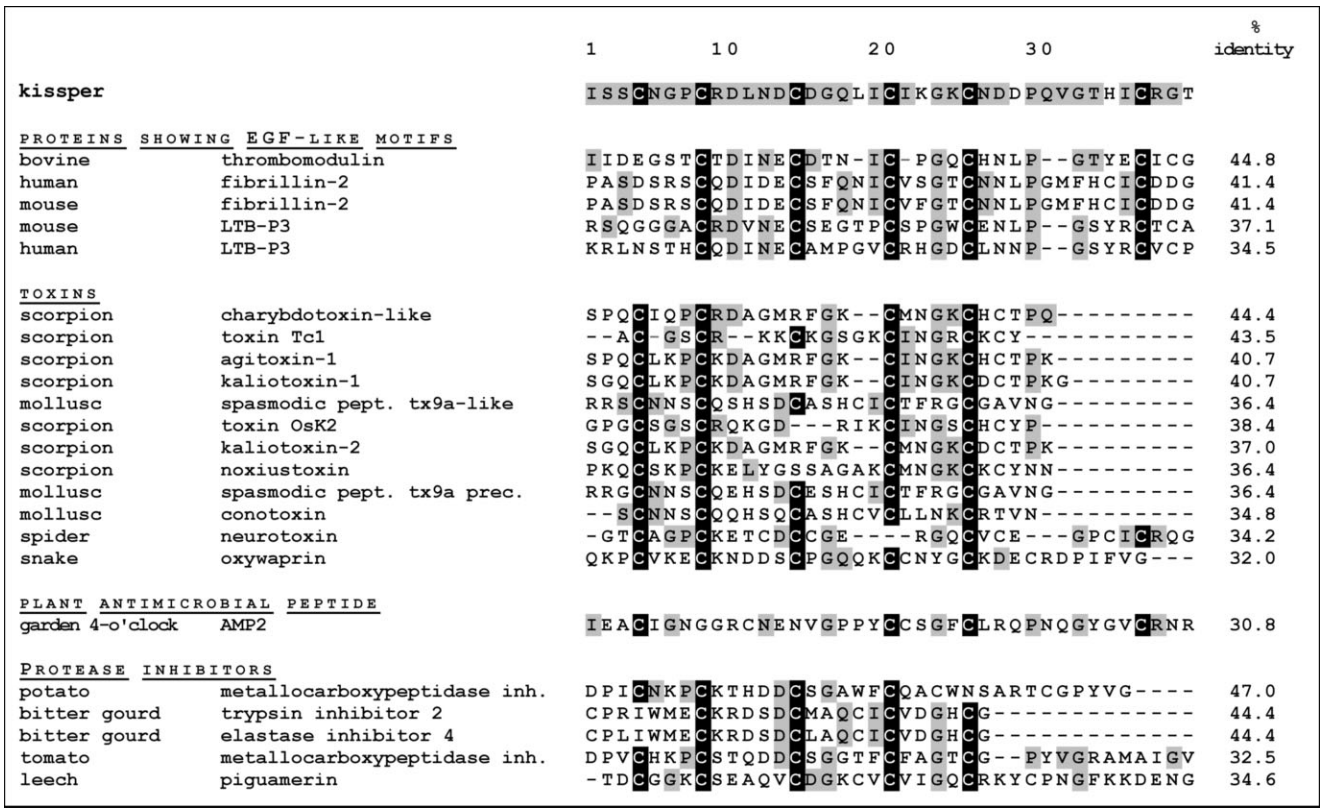

Figure 2 Alignment of the amino acid sequence of kissper with those of the most similar peptides and proteins available in the Swiss-Prot Data Bank, identified by the Fasta3 program. The cysteine residues of kissper conserved in other sequences are black-shadowed; other conserved residues are grey-shadowed. Accession numbers are the following: bovine thrombomodulin, P06579; human fibrillin-2 precursor, P35556; mouse fibrillin-2 precursor, Q61555; mouse latent transforming growth factor β-binding protein 3 precursor, Q61810; human latent transforming growth factor β-binding protein 3 precursor, Q9NS15; scorpion charybdotoxin-like peptide, P59886; scorpion toxin Tc1, P83243; scorpion agitoxin-1, P46110; scorpion kaliotoxin-1, Q9NII7; mollusc spasmodic peptide tx9a-like precursor, Q9GU57; scorpion toxin OsK2, P83244; scorpion kaliotoxin-2, P45696; scorpion noxiustoxin, P08815; mollusc spasmodic peptide tx9a precursor Q9GU58; mollusc conotoxin, P83390; spider neurotoxin PRTx32C1, P83904; snake oxywaprin, P83952; garden 4 o'clock antimicrobial peptide 2, P25404; potato metallocarboxypeptidase inhibitor, P01075; bitter gourd trypsin inhibitor 2, P10295; bitter gourd elastase inhibitor 4, P10296; tomato metallocarboxypeptidase inhibitor, P01076; leech piguamerin, P81499.

described above, for 20 h. Four peaks were obtained upon HPLC analysis (not shown). Both the peptides eluted at the retention times 26.9 and 27.4 min showed a single molecular mass in agreement with that derived from the entire sequence of kissper. The sample eluted at 25.2 min showed a single molecular mass of 1680 Da, and two amino acid sequences proceeding from Leu11 to Leu18 and from Gly23 to Asp28, respectively. This result allowed to clearly identify the disulfide bridge established between Cys14 and Cys25. The sample eluted at 25.9 min showed a single molecular mass of 2415 Da, and three amino acid sequences proceeding from Ile1 to Asp10, from Ile19 to Lys22 and from Pro29 to Arg37, respectively. This result (i) excluded disulfide bridges between Cys4 and Cys8 and between Cys20 and Cys36, and (ii) suggested two alternative disulfide bridge patterns, i.e. Cys4–Cys20/Cys8–Cys36 and Cys4–Cys36/Cys8–Cys20.

Solution Structure and Disulfide Bridges Connectivity

A conformational study was carried out by 2D NMR spectroscopy in a phosphate buffer solution at pH 3.5, i.e. at a pH value very close to that of both unripe and ripe kiwi fruit. Almost all proton signals were well resolved in the TOCSY experiment, but the β protons of the five aspartate, the three asparagine and the six cysteine residues were in a crowded spectral region. To overcome this problem, TOCSY, NOESY and ^{1}H-^{15}N-HNSQC spectra were acquired at different temperatures. Spin system identification of individual resonances and sequence specific assignment of kissper were carried out by the usual combination of TOCSY, DQF-COSY and NOESY spectra, according to the standard procedure [34]. The good dispersion of the NH chemical shifts, which can be diagnostic of the presence of nonrandom structures in solution, is well evident in the ^{1}H-^{15}N-HSQC spectrum reported in Figure 3(a) with the assignment of all amide resonances.

DOI: 10.1002/psc

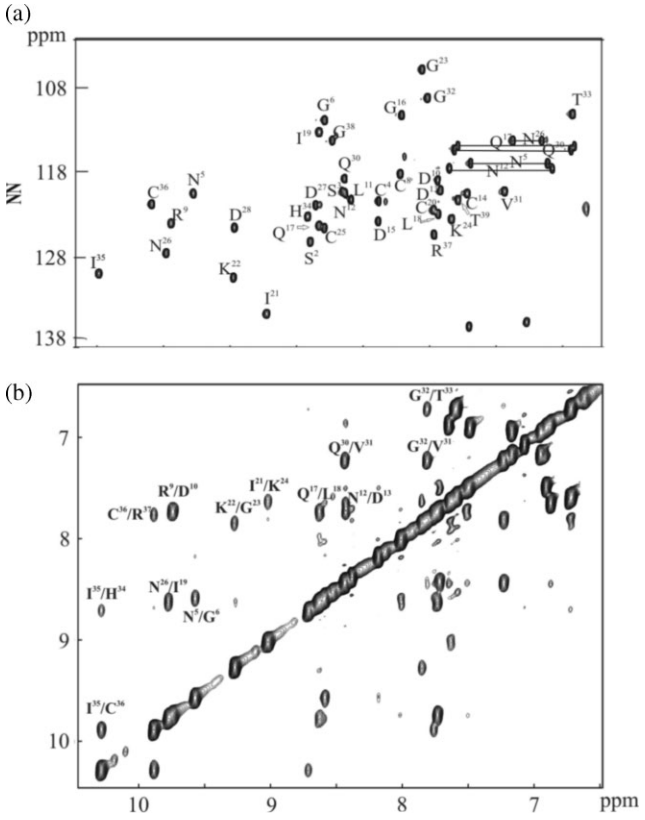

Figure 3 (a) ^{1}H-^{15}N HSQC spectrum of natural abundance 0.4 mM kissper in 25 mM phosphate buffer pH 3.5. Labels represent assignments for the cross peaks. The side chain -NH_2 amide protons of asparagine and glutamine residues are connected through horizontal lines. (b) Amide region of the 300 ms mixing time NOESY spectrum at 600 MHz on the sample of panel a. Cross peak labels identify inter-residue NOEs.

The proton assignment, reported in Table 1, was 97% complete, the missing resonances corresponding to Pro29 that could not be identified in the TOCSY or in the NOESY experiments, due to the strong overlap of resonances. The low field region of the NOESY spectrum with labeling of NH–NH connectivities is reported in Figure 3(b).

The careful analysis of NOESY data indicated that the peptide is characterized by the presence of multiple conformations, with almost all sequential d_{NN}(i, i + 1), typical of helical structures, alternated with strong $d_{\alpha N}$(i, i + 1), characteristic of extended structures. Nevertheless, the presence of several long-range effects, such as two d_{NN} involving residues 21–24 and 19–26, as well as a $d_{\alpha N}$ between residues 25–19 is consistent with the presence of a β-hairpin with the two short β-strands encompassing Ile19–Ile21 and Lys24–Asn26, connected through a central loop centered on Lys22–Gly23. Moreover, sequential d_{NN}(i, i + 1) in the *C*-terminal region in combination with d_{NN}(i, i + 2) and $d_{\alpha\beta}$ (i, i + 3), are indicative of a short helical stretch encopassing residues 32–35.

To define a plausible structure of kissper in aqueous environment, and also to facilitate the assignment of ambiguous NOE cross-peaks, preliminary structure calculations were performed with the DYANA package. A total of 237 upper distance limits were derived from the cross-peaks integrals of the NOESY spectrum at 300 ms mixing time, and five $^{3}J_{NH-\alpha CH}$ coupling constants values were extracted directly from the 1D proton spectrum, due to the good resolution of the related amide resonances.

Eighty structures were calculated from the refined list of structural constraints excluding disulfide bridges and dihedral angles constraints. As already described, the chemical characterization of disulfide bridges in kissper peptide allowed only the identification of a Cys14–Cys25 bridge. Since the Cys4–Cys8 and Cys20–Cys36 bridges were also excluded on the basis of biochemical data, to elucidate the two remaining disulfide bridges we repeated structural calculations considering all possible combinations of the remaining cysteine residues, i.e. either Cys4–Cys20/Cys8–Cys36 and Cys4–Cys36/Cys8–Cys20, keeping fixed the Cys14–Cys25 bridge. The best 20 structures, in terms of both target function and constraint violations, correspond to the disulfide bridges Cys4–Cys36 and Cys8–Cys20. However, on the basis of this preliminary NMR study, the alternative combination cannot be excluded. Figure 4 shows a representative structural model of kissper, with the secondary structure elements and the 4–36, 8–20 and 14–25 disulfide bridges pattern, as visualized by the program MOLMOL [35].

Insertion of Kissper into POPC and DOPS : DOPE : POPC PLM and Channel-Like Activity

In order to analyze the ability of kissper to induce ion conductance, PLMs of POPC and of DOPS : DOPE : POPC were used. Furthermore, the incorporation and pore formation of kissper as a function of pH were investigated in POPC PLM.

In five different experiments in POPC PLM, the addition of 0.04 μg/ml (10 nmol/l) of kissper to the *cis* side of the medium (KCl 1 M, pH 7.0) facing the membrane did not produce any conductance variation for a long period of time (>24 h), upon application of voltage as high as 140 mV (Figure 5(a)). In contrast, in experiments carried out at pH 3.5, step-like variations in membrane current compatible with single channel activity, were manifested in short time (about 13 min) when a constant voltage of 40 mV was applied to the membrane. This result was confirmed in new experiments carried out initially at pH 7.0, then lowering the pH to 3.5 by addition of a small amount of concentrated HCl solution, checking the pH during and at the end of the experiments.

Under all the responsive potentials tested, we observed alternating periods of bursting channel

DOI: 10.1002/psc

Table 1 Proton chemical shift values of 0.4 mM kissper in 25 mM phosphate buffer (in 90% H_2O, 10% ^2H_2O), at pH 3.5 and 300 K. The figures in square brackets report the ^{15}N chemical shifts of backbone amide nitrogens

Residues	HN [HN]	HC_α	HC_β	HC_γ	HC_δ	Others
Ile[1]	—	3.84	1.77	1.32–1.13	0.77	—
Ser[2]	8.69 [120.2]	4.68	4.09–3.63	—	—	—
Ser[3]	8.44 [114.4]	4.40	3.80	—	—	—
Cys[4]	8.18 [115.5]	3.80	2.73–2.80	—	—	—
Asn[5]	9.57 [114.5]	4.18	2.97	—	—	7.49–6.90
Gly[6]	8.59 [106.1]	3.58–4.39	—	—	—	—
Pro[7]	—	4.80	2.16–1.81	—	—	—
Cys[8]	8.02 [112.3]	4.65	3.13–2.95	—	—	—
Arg[9]	9.74 [118.0]	4.26	1.58	1.75	3.10	7.50
Asp[10]	7.73 [113.2]	4.22	2.74–2.88	—	—	—
Leu[11]	8.39 [114.4]	3.78	1.95–1.67	1.57	0.85	—
Asn[12]	8.43 [115.3]	4.70	2.73–2.84	—	—	7.65–6.88
Asp[13]	7.71 [114.2]	4.72	3.09–2.73	—	—	—
Cys[14]	7.51 [114.7]	5.11	2.52–2.73	—	—	—
Asp[15]	8.18 [117.8]	4.32	2.38	—	—	—
Gly[16]	8.01 [105.5]	3.68	—	—	—	—
Gln[17]	8.63 [118.4]	4.21	1.86	2.22	—	7.58–6.71
Leu[18]	7.75 [117.0]	4.20	1.79	1.15	0.65–0.48	—
Ile[19]	8.63 [107.4]	4.58	1.65	1.09–0.82	0.82	—
Cys[20]	7.76 [116.6]	4.67	2.74–2.16	—	—	—
Ile[21]	9.02 [128.6]	4.13	1.65	1.35–0.81	0.81	—
Lys[22]	9.28 [124.4]	3.70	1.90	1.34	1.72	—
Gly[23]	7.85 [100.1]	3.92	—	—	—	—
Lys[24]	7.63 [117.7]	5.21	1.58	1.10	1.33	—
Cys[25]	8.59 [118.6]	5.17	2.91–2.38	—	—	—
Asn[26]	9.77 [121.5]	4.90	2.68–2.48	—	—	7.17–6.95
Asp[27]	8.65 [116.0]	4.22	2.20–1.98	—	—	—
Asp[28]	9.26 [118.5]	4.62	2.49–3.03	—	—	—
Pro[29]	—	—	—	—	—	—
Gln[30]	8.44 [112.9]	4.05	2.03	2.27–2.33	—	—
Val[31]	7.23 [114.4]	3.96	2.15	0.93	—	—
Gly[32]	7.81 [103.5]	3.66–3.90	—	—	—	—
Thr[33]	6.72 [105.3]	3.98	4.20	1.06	—	—
His[34]	8.71 [117.3]	4.75	2.87–3.13	—	—	7.07–8.38
Ile[35]	10.29 [123.9]	3.70	1.91	1.51–1.09	0.76	—
Cys[36]	9.89 [115.9]	4.92	3.24–3.01	—	—	—
Arg[37]	7.76 [119.5]	4.24	1.80	1.58	3.08	7.07
Gly[38]	8.53 [108.4]	3.92	—	—	—	—
Thr[39]	7.58 [115.3]	4.06	—	1.06	—	—

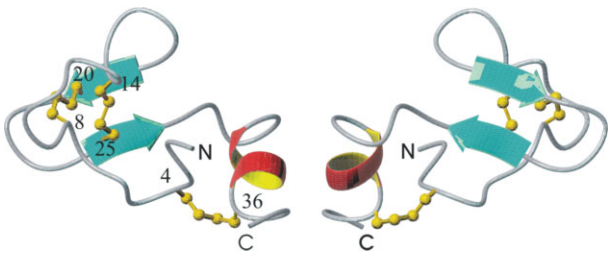

Figure 4 MOLMOL ribbon representation of a kissper solution structure as derived by structure calculations performed with DYANA package. The two models correspond to the front and rear views of the calculated structure. On the left model the labels evidence the pattern of the three disulfide bridges.

activity followed by quiescent periods in which a return of the current to the baseline was observed (Figure 5(b)). At pH 7.0, when the peptide concentration in the medium was doubled (0.08 μg/ml, corresponding to 20 nmol/l), the channel activity was elicited, in about 24 h, with an applied voltage of 80 mV, and could be registered at higher positive and negative voltages (Figure 5(c)). However, for applied voltage higher than ±120 mV the membrane, after a high rate of channel formation, resulted destabilized. In the same experimental conditions, but at pH 3.5, the channel activity was triggered by a lower applied potential (20 mV) and arised in a shorter time (about 9 min).

DOI: 10.1002/psc

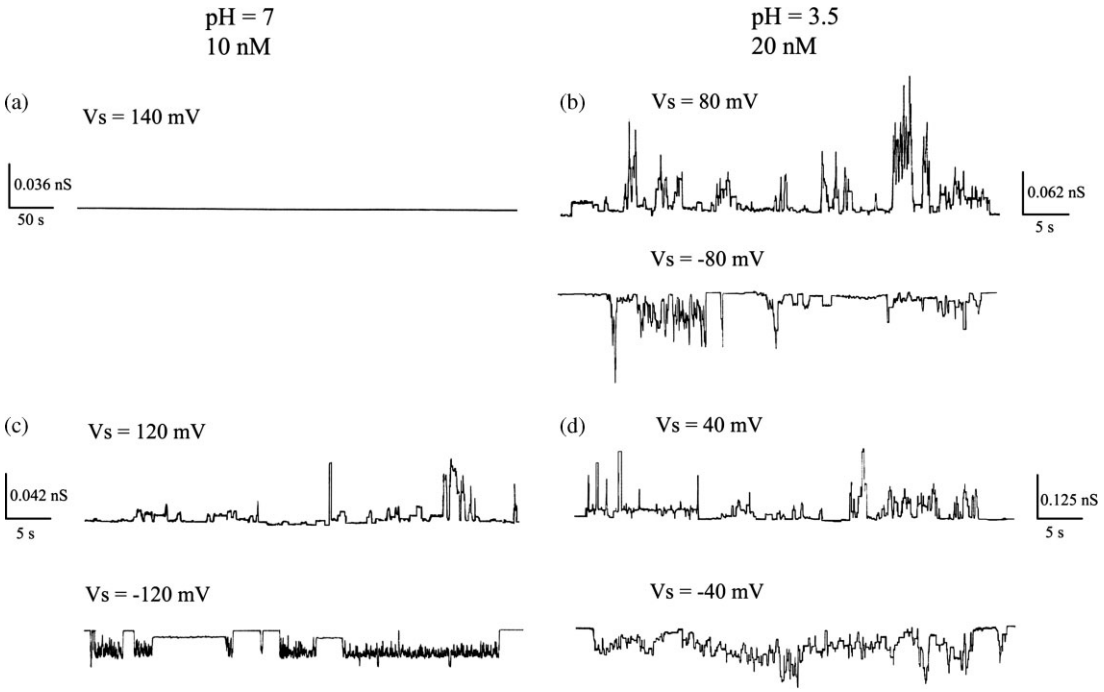

Figure 5 Chart recordings of kissper channel formation in POPC PLM at different pH values of the medium (a and c, pH = 7.0; b and d, pH = 3.5), at various holding potential (indicated on the top of the tracing), and at different kissper concentrations (a and b, 0.04 μg/ml; c and d, 0.08 μg/ml). Channel opening and closing are represented by upward/downward (for positive applied voltage) or downward/upward (for negative applied voltage) deflections, respectively. Each trace represents a fragment of the recorded activity obtained in individual experiments at different times. Experimental conditions: 1 M KCl; kissper was present on the *cis* side of the membrane; temperature was 22 °C.

Furthermore, in these conditions the channel activity was paroxystic and even at low potential the count of the total number of single-channel-like events was difficult (Figure 5(d), −40 mV). An increasing in the potential resulted in an irreparable destabilization of the membrane.

In order to test the effect of membrane composition upon kissper incorporation and channel-like activity, a PLM made up of DOPS : DOPE : POPC (27 : 27:18, w : w : w) was used. This membrane is characterized by the presence of the net negative charge of DOPS and of the neutral DOPE, a nonlamellar-forming lipid. Experiments carried out by using DOPS : DOPE : POPC PLM at pH 7.0, upon addition of 0.04 μg/ml of kissper on the *cis* side, showed channel-like activity when a constant voltage of 80 mV was applied (Figure 6(a)). The range of channel-like activity registered was very high (from 60 to 140 mV), and the peptide addition stabilized the membrane even at potential values higher than 140 mV, although the conductance events were not observed. By doubling the kissper concentration (0.08 μg/ml), the voltage at which the pore-forming activity arised was lower (60 mV) and the range of channel-like activity reduced (from 20 to 60 mV and from −20 to −40 mV) (Figure 6(b)). In this case, higher positive or negative applied voltages induced a paroxystic pore-forming activity that in a short time (minutes) broke the membrane, thus precluding the possibility to calculate channel-like activity (Figure 6(c)).

All single events were used to calculate the channel amplitude. Current amplitudes analyzed in the different experiments revealed the existence of one main conductance level. The central value of the single-channel conductance ± SE was obtained by constructing a histogram of the amplitude distribution and fitting the data by a Gaussian distribution function (Figure 7).

Table 2 summarizes the results obtained under different experimental conditions and with both PLMs. In particular, the Table shows (i) the activation voltage, i.e. the lowest applied voltage that induces channel-like activity across membrane, (ii) the activation time, i.e. the time at which the first conductance variation is evident after kissper addition, (iii) the range of activity, i.e. the range of the applied voltages to detect channel-like activity, (iv) the central conductance ($\Lambda_c \pm$ SE), (v) the channel occurrence frequency, i.e. the mean number of openings in a period of 60 s, (vi) the total number of events, and (vii) the effect of kissper on membrane stability. All data are reported as a function of membrane composition, pH variation and kissper concentration. The analysis of the lifetime of the channel with the known equation [30] was difficult as the events were preponderant over the terminating events, the latter being less than 100 (minimum number of channels for an appropriate

DOI: 10.1002/psc

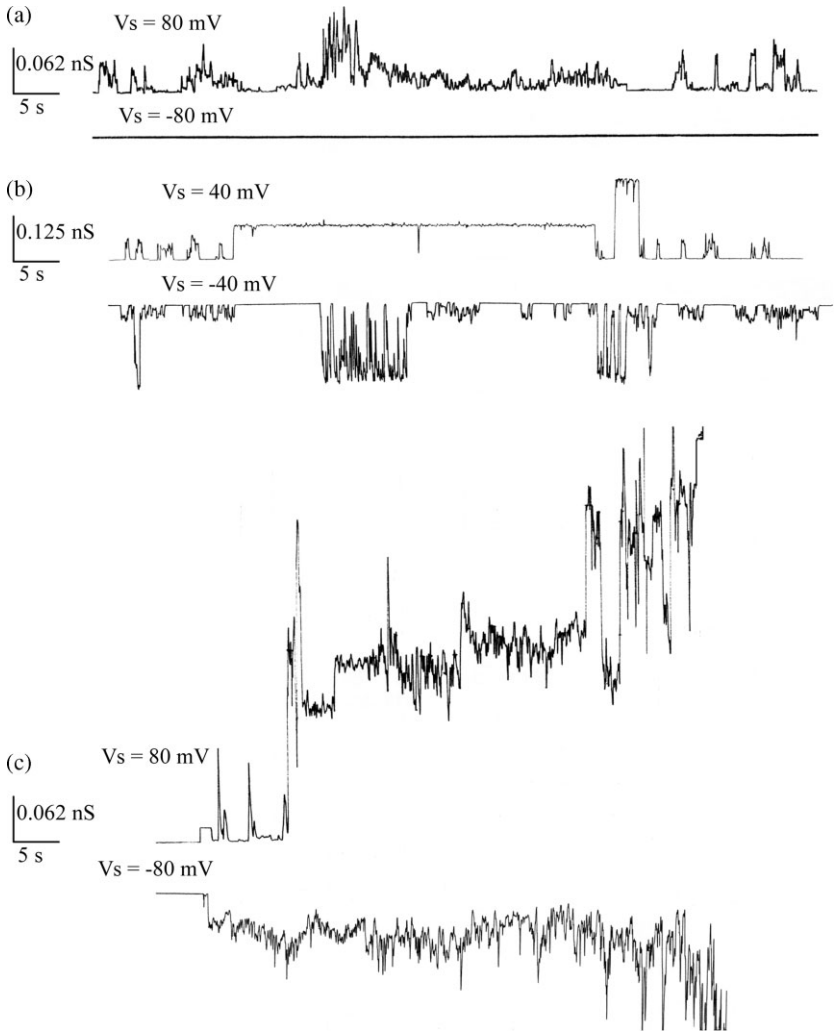

Figure 6 Chart recordings of kissper channel formation in DOPS : DOPE : POPC PLM at various holding potential (indicated on the top of the tracing), and at different kissper concentrations (a, 0.04 μg/ml; b and c, 0.08 μg/ml). Channel opening and closing are represented by upward/downward (for positive applied voltage) or downward/upward (for negative applied voltage) deflections, respectively. Each trace represents a fragment of the recorded activity obtained in individual experiments at different times. Experimental conditions: 1 M KCl; kissper was present on the *cis* side of the membrane; pH 7.0; temperature was 22 °C.

statistics). However, the duration of the observed channels, although variable (see Figures 5 and 6), and despite the different PLMs, pH or kissper concentration used, was within a similar lifetime range (from 0.85 to 15.75 s).

It can be observed that the kissper channel-like activity can be affected by both PLM composition and pH conditions. In all the experimental conditions used, kissper channel conductance resulted potential-dependent, independently of both the pH value of POPC PLM and the membrane composition (Figure 8).

In POPC PLM (at different pH values) and in DOPS : DOPE : POPC PLM (at pH 7.0), the ion selectivity of the channel was determined in asymmetrical conditions, i.e. in the presence of a salt gradient. At zero current value, the voltage difference represents the reversal potential. Approximately the same result was obtained with I–V curve, where the measured amplitude of the channel events at each membrane potential was used to calculate the reversal potential. In this case for kissper channels in POPC PLM at pH 7.0 and 3.5, in an asymmetrical condition of KCl concentration of 1.5–0.3 M and 1.5–1.0 M *cis*/*trans* side respectively, the reversal potential was 5.76 and 5.38 mV, giving, by using the Goldman-Hodgkin-Katz equation, a calculated P_{K^+}/P_{Cl^-} of 0.71 and 0.31, respectively. In DOPS : DOPE : POPC membrane, in an asymmetrical concentration of KCl of 1.0–0.5 M *cis*/*trans* at pH 7.0, the reversal potential of kissper channel was 6.24 mV giving a calculated P_{K^+}/P_{Cl^-} of 0.47.

DISCUSSION

Kissper is a 39-residue peptide isolated in good yield from the edible part of kiwi fruit, whose amino acid

DOI: 10.1002/psc

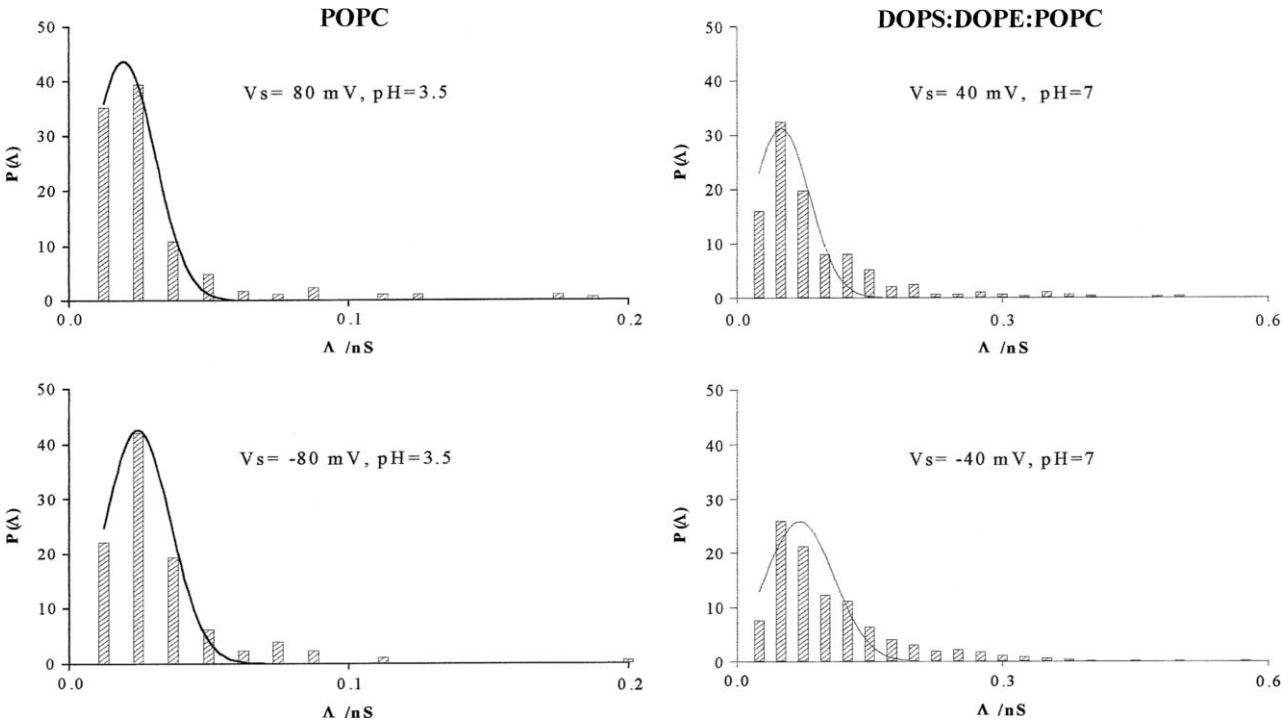

Figure 7 Amplitude histograms of kissper channel conductance relative to the experiments reported in Figures 5 and 6. The histogram of the probability [P(Λ)] for the occurrence of a given conductivity unit was fitted by a Gaussian, which is shown as a solid curve.

sequence showed 100% identity with the first 39 residues of the *N*-terminal region of kiwellin, the allergenic protein previously isolated from the same source and characterized [17]. Therefore, it may be hypothesized that kissper derives from the processing of the precursor kiwellin, through the cleavage of the peptide bond between Thr39 and Thr40.

Kissper, as well as the entire sequence of the precursor kiwellin, has a very high identity with the putative kiwellin from potato leaves (UNIPROT accession number Q2HPL5), and the cDNA-derived sequence of the hypothetical protein Grip22 from grape [32], whose mRNA is differentially expressed during fruit ripening. However, no information about the function of kiwellin and both the homologous proteins from grape and potato is so far available.

Homology search and comparative analysis of fold prediction showed a rather low structural similarity of kissper with other peptides and proteins with known function. However, kissper showed a cysteine pattern similar to those observed in proteins and peptides displaying the so-called EGF-like cysteine-rich motif [33], such as mammalian fibrillins, scorpion, snake and insect toxins, human endothelins, protease inhibitors, and antimicrobial peptides. Four or five cysteine residues out of the six of kissper sequence are indeed conserved in peptides and proteins belonging to these classes. Literature reports describe structural similarities between polypeptides showing the EGF-like motif and plant pore-forming peptides, including thionins and defensins, which are involved in defence mechanisms against pathogens [6,8,36].

The observation that most of these polypeptides display their function by interacting with membrane lipids or proteins [6,33,37,38] suggested a possible similar action mechanism for kissper. Attempts to test the kissper channel blocker activity provided unclear preliminary results (data not shown). In contrast, clear results were obtained when the kissper capacity to permeabilize synthetic membranes was tested. In fact, reconstitution of kissper in PLMs of both POPC, an ubiquitary plasma membrane phospholipid, and DOPS : DOPE : POPC, a surrogate of intestinal membrane, revealed peptide incorporation and channel-like activity. However, PLM composition affected the pore-forming activity that also showed concentration and voltage dependence. In both PLM systems tested, anion selectivity was observed. Kissper showed efficient incorporation into PLMs and ion channeling at concentration values generally lower than those reported for several pore-forming peptides, such as defensins, thionins, cecropins, cryptidin, duramycin, etc [39–43]. Furthermore, the channel-like activity of kissper was markedly affected by pH conditions. At neutral pH values, the ion transport was observed only within a limited range of experimental conditions. In contrast, under acidic pH conditions, in POPC PLM the channel-like activity was more efficient and the ion transport occurred even at voltage and peptide concentration ineffective at neutral pH. Furthermore,

DOI: 10.1002/psc

Table 2 Planar lipid membrane observations on kissper

PLM pH	Kissper (μg/ml)	Activ. voltage (mV)	Activ. time(min)	Range of activity (mV)	Λ_c at 80 mV (nS ± SE)	Lifetime channels (sec)	Occur. (even./min) ± SD	N events	Effect on membrane stability
POPC 3.5	0.04	40	13	±40 ÷ ±100	0.02 ± 0.0007	0.75 ÷ 12.2	0.96 ± 0.07	165	Unstable for Vs > ± 100 mV
POPC 7.0	0.08	80	1440	±60 ÷ ±120	0.025 ± 0.001	0.75 ÷ 17.2	1.77 ± 0.14	167	Unstable for Vs > ± 120 mV
POPC 3.5	0.08	20	9	±40 ÷ ±80	0.024 ± 0.001	0.75 ÷ 18.7	5.26 ± 0.03	367	Unstable for Vs > ± 80 mV
DOPS : DOPE : POPC 7.0	0.04	80	11	+60 ÷ +140	0.019 ± 0.001	0.75 ÷ 16.7	1.73 ± 0.11	255	Stable for Vs > ± 140 mV
DOPS : DOPE : POPC 7.0	0.08	60	180	+20 ÷ +60 − 20 ÷ −40	0.054 ± 0.003[a]	1.25 ÷ 13.7	2.69 ± 0.18	249	Unstable for Vs > − 40 and Vs > + 60 mV

[a] The central conductance is referred to an applied voltage of 60 mV.

at low pH the anion selectivity of the pores became much more marked.

It is worth recalling that an acidic-pH dependence of cytotoxicity and, in particular, of *in vitro* channel-forming activity has been described for other peptides [44,45] and for large toxins or toxin-like molecules [46–48]. A low-pH activation has been reported, for example, for bacteriocins, such as the *Escherichia coli* colicin E1, for the diphtheria, anthrax and cholera toxins [49], and for *Bacillus thuringiensis* toxins [50]. The acidic-pH dependence of these activities has been explained by assuming that the protonated state of one or more acidic amino acid side-chain(s) is a requirement for channel formation, membrane insertion and voltage gating [46]. Three aspartic residues (Asp408, Asp410, and Asp423) in the colicin E1 channel domain have been involved in critical pH-sensitive conformational transition of the activation process [49]. Intriguingly, kissper has five aspartic residues, and three of them are arranged into a Asp-Xaa-Asp-Xaa(12)-Asp pattern, similar to that observed in colicin E1. However, this hypothesis could be proved only by evaluating the effects of mutant peptides on the same processes or, alternatively, by performing an extensive characterization of the 3D structure of kissper in different environments. At the moment, we have undertaken a conformational study of this peptide in solution by 2D NMR. Preliminary results under acidic conditions (pH 3.5) in aqueous buffer and at a temperature of 300 K indicated that kissper, like many other typical disulfide-rich small proteins [51], shows a quite flexible 3D structure, despite the presence of the conformational constraints imposed by three disulfide

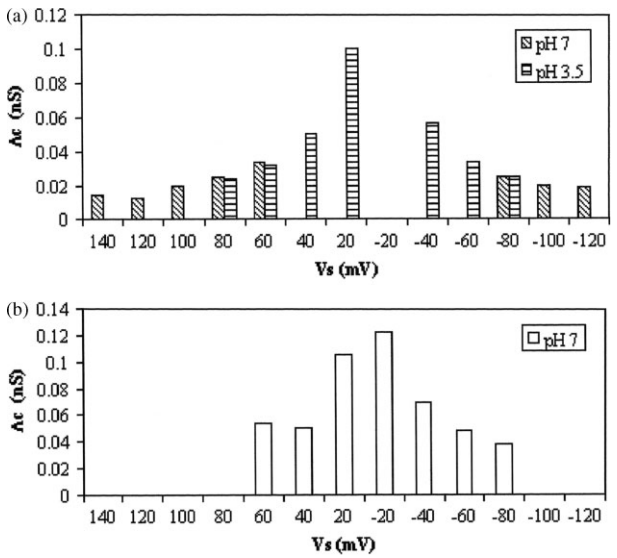

Figure 8 Conductance–voltage relationship for kissper channels at pH 7.0 and pH 3.5 in POPC (a) and at pH 7.0 in DOPS : DOPE : POPC (b) PLM. Experimental conditions: 1 M KCl; 0.08 μg/ml kissper, present on the *cis* side of POPC membrane; temperature was 22 °C.

DOI: 10.1002/psc

bridges involving the six cysteine residues, with only a small amount of regular secondary structure. A careful analysis of the NMR derived structures allowed the identification of a sizeable amount of molecules with short secondary structure elements that can be described as a short antiparallel β-sheet encompassing residues 19–21/24–26 and a short helix spanning residues 32–35. We believe that this helical stretch is unable to span a bilayer to form channels, for which perhaps an aggregate of molecules is necessary. However, a model for kissper pore structure cannot be described in the light of the existing data. For this purpose, it will be necessary to perform extensive characterization of kissper 3D structure under different biomimetic conditions.

The comparative analysis of the structural and functional properties of kissper suggested that, despite the similarities observed with a variety of large and small toxins and, in general, with proteins containing the EGF-like motif, it cannot be included in any of the known peptide families. Plant thionins, for instance, are cationic peptides of 45–54 residues, with eight conserved cysteine residues forming four intramolecular disulfide bridges [7,52] and with a typical 3D structure characterized by the so-called cysteine-stabilized $\alpha\beta$ motif [53], i.e. a triple-stranded antiparallel β-sheet connected to an α-helix through a disulfide bridge. Moreover, α-defensins, which have the same I–VI, II–IV, III–V cysteine pairing proposed for kissper, show a different size of the Cx_nC segments, are smaller than kissper, cationic, and are characterized by triple-stranded antiparallel β-sheet structures [54].

Kissper is a small, anionic, cysteine-rich member of a new family of peptides with pH-dependent and voltage-gated pore-forming activity, characterized by anion selectivity and channeling. Beyond the physiological role in the plant cell, the capacity of this food peptide to form channel-like pathways in a lipid bilayer, whose composition is similar to that found in intestinal cells, suggests potential biological effects on human health. The high amount of kissper found in ripe kiwi fruit and its strong resistance to proteolysis suggest that it could very likely affect the gastrointestinal physiology. In perspective, experiments on isolated intestinal tissue and, possibly, *in vivo* studies, will allow the characterization of the local and of possible systemic effects of kissper.

Furthermore, kissper functional properties suggest a potential pharmacological use of this peptide as it is or after appropriate modifications, for the treatment of pathologies involving nonoptimal ion transport mechanisms. For example, defective anion channels have been related to many pathologies, such as cystic fibrosis [55–57], for which channel replacement therapy has been proposed as a possible treatment [43]. In this context, peptides forming anionic channels may assume physiological relevance for the biological functions related to the ionic balance through the cell.

Acknowledgements

This work received financial support from MIUR (FIRB RBNE03B8KK).

REFERENCES

1. Roberfroid MB. Concepts in functional foods: the case of inulin and oligofructose. *J. Nutr.* 1999; **129**: 1398S–1401S.
2. Rutherfurd-Markwick KJ, Moughan PJ. Bioactive peptides derived from food. *J. AOAC Int.* 2005; **88**: 955–966.
3. Hartmann R, Meisel H. Food-derived peptides with biological activity: from research to food applications. *Curr. Opin. Biotechnol.* 2007; **18**: 163–169.
4. Eastwood MA. A molecular biological basis for the nutritional and pharmacological benefits of dietary plants. *Q. J. Med.* 2001; **94**: 45–48.
5. Kitts DD, Weiler K. Bioactive proteins and peptides from food sources. Applications of bioprocesses used in isolation and recovery. *Curr. Pharm. Des.* 2003; **9**: 1309–1323.
6. Froy O, Gurevitz M. Membrane potential modulators: a thread of scarlet from plants to humans. *FASEB J.* 1998; **12**: 1793–1796.
7. Almeida MS, Cabral KMS, Kurtenbach E, Almeida FCL, Valente AP. Solution structure of Pisum sativum defensin 1 by high resolution NMR: plant defensins, identical backbone with different mechanisms of action. *J. Mol. Biol.* 2002; **315**: 749–757.
8. Anaya-Lopez JL, Lopez-Meza JE, Baizabal-Aguirre VM, Cano-Camacho H, Ochoa-Zarzosa A. Fungicidal and cytotoxic activity of a Capsicum chinense defensin expressed by endothelial cells. *Biotechnol. Lett.* 2006; **28**: 1101–1108.
9. Motohashi N, Shirataki Y, Kawase M, Tani S, Sakagami H, Satoh K, Kurihara T, Nakashima H, Mucsi I, Varga A, Molnar J. Cancer prevention and therapy with kiwifruit in Chinese folklore medicine: a study of kiwifruit extracts. *J. Ethnopharmacol.* 2002; **81**: 357–364.
10. Collins AR, Harrington V, Drew J, Melvin R. Nutritional modulation of DNA repair in a human intervention study. *Carcinogenesis* 2003; **24**: 511–515.
11. Jung K-A, Song T-C, Han D, Kim I-H, Kim Y-E, Lee C-H. Cardiovascular protective properties of kiwifruit extracts in vitro. *Biol. Pharm. Bull.* 2005; **28**: 1782–1785.
12. Rush EC, Patel M, Plank LD, Ferguson LR. Kiwifruit promotes laxation in the elderly. *Asia Pac. J. Clin. Nutr.* 2002; **11**: 164–168.
13. Gavrovic-Jankulovic M, Cirkovic T, Vuckovic O, Atanaskovic-Markovic M, Petersen A, Gojgic G, Burazer L, Jankov RM. Isolation and biochemical characterization of a thaumatin-like kiwi allergen. *J. Allergy Clin. Immunol.* 2002; **110**: 805–810.
14. Pastorello EA, Conti A, Pravettoni V, Farioli L, Rivolta F, Ansaloni R, Ispano M, Incorvaia C, Giuffrida MG, Ortolani C. Identification of actinidin as the major allergen of kiwi fruit. *J. Allergy Clin. Immunol.* 1998; **101**: 531–537.
15. Lucas JSA, Lewis SA, Hourihane JOB. Kiwi fruit allergy: a review. *Pediatr. Allergy Immunol.* 2003; **14**: 420–428.
16. Bublin M, Mari A, Ebner C, Knulst A, Scheiner O, Hoffmann-Sommergruber K, Breiteneder H, Radauer C. IgE sensitization profiles toward green and gold kiwifruits differ among patients allergic to kiwifruit from 3 European countries. *J. Allergy Clin. Immunol.* 2004; **114**: 1169–1175.
17. Tamburrini M, Cerasuolo I, Carratore V, Stanziola AA, Zofra S, Romano L, Camardella L, Ciardiello MA. Kiwellin, a novel protein from kiwi fruit. Purification, biochemical characterization and identification as an allergen. *Protein J.* 2005; **24**: 423–429.

18. Camardella L, Carratore V, Ciardiello MA, Servillo L, Balestrieri C, Giovane A. Kiwi protein inhibitor of pectin methylesterase. Amino-acid sequence and structural importance of two disulfide bridges. *Eur. J. Biochem.* 2000; **267**: 4561–4565.
19. Ciardiello MA, Tamburrini M, Tuppo L, Carratore V, Giovane A, Mattei B, Camardella L. Pectin methylesterase from kiwi and kaki fruits: purification, characterization and role of pH in the enzyme regulation and interaction with the kiwi proteinaceous inhibitor. *J. Agric. Food Chem.* 2004; **52**: 7700–7703.
20. Schwarz S, Hostetler B, Ling S, Mone M, Waltkins J. Intestinal membrane lipid composition and fluidity during development in the rat. *Am. J. Physiol.* 1985; **248**: G200–G207.
21. Cavanagh J, Rance M. Suppression of cross-relaxation effects in TOCSY spectra via a modified DIPSI-2 mixing sequence. *J. Magn. Reson.* 1992; **96**: 670–678.
22. Jeener J, Meyer BH, Bachman P, Ernst RR. Investigation of exchange processes by two-dimensional nmr spectroscopy. *J. Chem. Phys.* 1979; **71**: 4546–4553.
23. Rance M, Sørensen OW, Bodenhausen G, Wagner G, Ernst RR, Wüthrich K. Improved spectral resolution in COSY 1H NMR spectra of proteins via double quantum filtering. *Biochem. Biophys. Res. Commun.* 1983; **117**: 479–485.
24. Bax A, Ikura M, Kay LE, Torchia DA, Tschudin R. Comparison of different modes of two-dimensional reverse correlation NMR for the study of proteins. *J. Magn. Reson.* 1990; **86**: 304–318.
25. Piotto M, Saudek V, Sklenar V. Gradient-tailored excitation for single-quantum NMR spectroscopy of aqueous solutions. *J. Biomol. NMR* 1992; **2**: 661–666.
26. Delaglio F, Grzesiek S, Vuister G, Zhu G, Pfeifer J, Bax A. NMRPipe: A multidimensional spectral processing system based on UNIX pipes. *J. Biomol. NMR* 1995; **6**: 277–293.
27. Johnson BA, Blevins RA. NMR View: a computer program for the visualization and analysis of NMR data. *J. Biomol. NMR* 1994; **4**: 603–614.
28. Wishart DS, Bigam CG, Yao J, Abildgaard F, Dyson HJ, Oldfield E, Markley JL, Sykes BD. 1H, 13C and 15N chemical shift referencing in biomolecular NMR. *J. Biomol. NMR* 1995; **6**: 135–140.
29. Güntert P, Mumenthaler C, Wüthrich K. Torsion angle dynamics for NMR structure calculation with the new program DYANA. *J. Mol. Biol.* 1997; **273**: 283–298.
30. Micelli S, Meleleo D, Picciarelli V, Gallucci E. Effect of sterols on beta-amyloid peptide (AbetaP 1–40) channel formation and their properties in planar lipid membranes. *Biophys. J.* 2004; **86**: 2231–2237.
31. Hill B. Selective permeability: impedence. *Ion Channels of Excitable Membranes*. Sinauer Associated, Inc. Publishers: Sunderland, MA, 2001; 441–470.
32. Davies C, Robinson SP. Differential screening indicates a dramatic change in mRNA profiles during grape berry ripening. Cloning and characterization of cDNAs encoding putative cell wall and stress response proteins. *Plant Physiol.* 2000; **122**: 803–812.
33. Oka T, Murata Y, Nakanishi T, Yoshizumi H, Hayashida H, Ohtsuki Y, Toyoshima K, Hakura A. Similarity, in molecular structure and function, between the plant toxin purothionin and the mammalian pore-forming proteins. *Mol. Biol. Evol.* 1992; **9**: 707–715.
34. Wüthrich K. *NMR of Proteins and Nucleic Acids*. Wiley: New York, 1986.
35. Koradi R, Billeter M, Wüthrich K. MOLMOL: a program for display and analysis of macromolecular structure. *J. Mol. Graph.* 1996; **14**: 51–55.
36. Pelegrini PB, Franco OL. Plant γ-thionins: Novel insights on the mechanism of action of a multi-functional class of defense proteins. *Int. J. Biochem. Cell Biol.* 2005; **37**: 2239–2253.
37. Xu CQ, Brone B, Wicher D, Bozkurt O, Lu WY, Huys I, Han YH, Tytgat J, Van Kerkhove E, Chi CW. BmBKTx1, a novel Ca2+-activated K+ channel blocker purified from the Asian scorpion Buthus martensi Karsch. *J. Biol. Chem.* 2004; **279**: 34562–34569.
38. Barona J, Batista CV, Zamudio FZ, Gomez-Lagunas F, Wanke E, Otero R, Possani LD. Proteomic analysis of the venom and characterization of toxins specific for Na+ and K+ channels from the Colombian scorpion Tityus pachyurus. *Biochim. Biophys. Acta* 2006; **1764**: 76–84.
39. Thevissen K, Ghazi A, De Sablanx GW, Brownlee C, Osborn RW, Broekaert WF. Fungal membrane responses induced by plant defensins and thionins. *J. Biol. Chem.* 1996; **21**: 15018–15025.
40. Wu M, Maier E, Benz R, Hancock REW. Mechanism of interaction of different classes of cationic antimicrobial peptides with planar bilayers and with the cytoplasmic membrane of Escherichia coli. *Biochemistry* 1999; **38**: 7235–7242.
41. Hughes P, Dennis E, Whitcross M, Llewellyn D, Gage P. The cytotoxic plant protein, b-purothionin, forms ion channels in lipid membranes. *J. Biol. Chem.* 2000; **14**: 823–827.
42. Yue G, Merlin D, Selsted ME, Lencer WI, Mafdara JL, Eaton DC. Cryptin 3 forms anion selective channels in cytoplasmic membranes of human embryonic kidney cells. *Am. J. Physiol. Gastrointest. Liver Physiol.* 2002; **282**: G757–G765.
43. Zeitlin PL, Boyle MP, Guggino WB, Molina L. A phase I trial of intranasal Moli1901 for cystic fibrosis. *Chest* 2004; **125**: 143–149.
44. Micelli S, Meleleo D, Picciarelli V, Gallucci E. Effect of pH-variation on insertion and ion channel formation of human calcitonin into planar lipid bilayers. *Front. Biosci.* 2006; **11**: 2035–2044.
45. Meleleo D, Gallucci E, Picciarelli V, Micelli S. Acetyl-[Asn^{30},Tyr^{32}]-calcitonin fragment 8–32 forms channels in phospholipid planar lipid membranes. *Eur. Biophys. J.* 2007; **36**: 763–770.
46. Shiver JW, Cramer WA, Cohn FS, Bishop LJ, de Jong PJ. On the explanation of the acidic pH requirement for in vitro activity of colicin E1. Site-directed mutagenesis at Glu-468. *J. Biol. Chem.* 1987; **262**: 14273–14281.
47. Oh KJ, Senzel L, Collier RJ, Finkelstein A. Translocation of the catalytic domain of diphtheria toxin across planar phospholipid bilayers by its own T domain. *PNAS* 1999; **96**: 8467–8470.
48. Zakharov SD, Lindeberg M, Griko Y, Salamon Z, Tollin G, Prendergast FG, Cramer WA. Membrane-bound state of the colicin E1 channel domain as an extended two-dimensional helical array. *PNAS* 1998; **95**: 4282–4287.
49. Musse AA, Merrill AR. The molecular basis for the pH-activation mechanism in the channel-forming bacterial colicin E1. *J. Biol. Chem.* 2003; **278**: 24491–24499.
50. Puntheeranurak T, Uawithya P, Potvin L, Angsuthanasombat C, Schwartz JL. Ion channels formed in planar lipid bilayers by the dipteran-specific Cry4B Bacillus thuringiensis toxin and its alpha1-alpha5 fragment. *Mol. Membr. Biol.* 2004; **21**: 67–74.
51. Harrison PM, Sternberg MJE. The disulphide beta-cross: from cystine geometry and clustering to classification of small disulphide-rich protein folds. *J. Mol. Biol.* 1996; **264**: 603–623.
52. Li S-S, Gullbo J, Lindholm P, Larsson R, Thunberg E, Samuelsson G, Bohlin L, Claeson P. Ligatoxin B, a new cytotoxic protein with a novel helix-turn-helix DNA-binding domain from the mistletoe Phoradendron liga. *Biochem. J.* 2002; **366**: 405–413.
53. White SH, Wimley WC, Selsted ME. Structure, function, and membrane integration of defensins. *Curr. Opin. Struct. Biol.* 1995; **4**: 521–527.
54. De Smet K, Contreras R. Human antimicrobial peptides: defensins, cathelicidins and histatins. *Biotechnol. Lett.* 2005; **27**: 1337–1347.
55. Du D, Sharma M, Lukacs GL. The DeltaF508 cystic fibrosis mutation impairs domain-domain interactions and arrests post-translational folding of CFTR. *Nat. Struct. Mol. Biol.* 2005; **12**: 17–25.
56. Shank LP, Broughman JR, Takeguchi W, Cook G, Robbins AS, Hahn L, Radke G, Iwamoto T, Schultz BD, Tomich JM. Redesigning channel-forming peptides: amino acid substitutions that enhance rates of supramolecular self-assembly and raise ion transport activity. *Biophys. J.* 2006; **90**: 2138–2150.
57. Gadsby DC, Vergani P, Csanady L. The ABC protein turned chloride channel whose failure causes cystic fibrosis. *Nature* 2006; **440**: 477–483.